Article ID: 1006-8775(2018) 03-0346-10

# CLOUD RADIATIVE AND MICROPHYSICAL EFFECTS ON THE RELATION BETWEEN SPATIAL MEAN RAIN RATE, RAIN INTENSITY AND FRACTIONAL RAINFALL COVERAGE

ZHANG Xiao-yi (张晓怡)[1, 2], ZHANG Zi-han (张子涵)[1, 3], LI Xiao-fan (李小凡)[1]

(1. Department of Atmospheric Sciences, School of Earth Sciences, Zhejiang University, Hangzhou 310027 China; 2. Airlines Operations Center, Xiamen Air, Hangzhou 311207 China; 3. Zhejiang Province Meteorological Observatory, Hangzhou 310017 China)

**Abstract:** Cloud radiative and microphysical effects on the relation between spatial mean rain rate, rain intensity and fractional rainfall coverage are investigated in this study by conducting and analyzing a series of two-dimensional cloud resolving model sensitivity experiments of pre-summer torrential rainfall in June 2008. The analysis of time-mean data shows that the exclusion of radiative effects of liquid clouds reduces domain mean rain rate by decreasing convective rain rate mainly through the reduced convective-rainfall area associated with the strengthened hydrometeor gain in the presence of radiative effects of ice clouds, whereas it increases domain mean rain rate by enhancing convective rain rate mainly via the intensified convective rain intensity associated with the enhanced net condensation in the absence of radiative effects of ice clouds. The removal of radiative effects of ice clouds decreases domain mean rain rate by reducing stratiform rain rate through the suppressed stratiform rain intensity related to the suppressed net condensation in the presence of radiative effects of liquid clouds, whereas it increases domain mean rain rate by strengthening convective rain rate mainly via the enhanced convective rain intensity in response to the enhanced net condensation in the absence of radiative effects of liquid clouds. The elimination of microphysical effects of ice clouds suppresses domain mean rain rate by reducing stratiform rain rate through the reduced stratiform-rainfall area associated with severely reduced hydrometeor loss.

**Key words:** pre-summer torrential rainfall; radiative effects of liquid and ice clouds; rain rate; rain intensity; fractional rainfall coverage

**CLC number:** P456.7 **Document code:** A

doi: 10.16555/j.1006-8775.2018.03.008

## 1 INTRODUCTION

The torrential rainfall events during pre-summer rainy season (usually taking place in April, May and June every year) over the south of China are important sources for regulating local hydrological cycle, but associated floods could cause serious social and economic consequences. Thus, forecasts for such heavy rainfall events are crucial, which rely on numerical weather modeling. The improvement of numerical modeling depends on understanding of physical processes that are responsible for formation and development of pre-summer torrential rainfall. Such studies have been conducted over decades (e.g., Krishnamurti et al.[1]; Tao and Ding [2]; Wang and Li[3]; Ding [4]; Simmonds et al.[5]). Lou et al.[6] revealed the important contributions of condensation to the increases in liquid hydrometeors and atmospheric temperature for the development of the pre-summer rainfall system. They also found that pre-summer rainfall starts with warm rain processes and is followed by cold rain processes when the melting of ice hydrometeors into rain becomes important. Shen et al.[7] showed that the exclusion of vertical wind shear increases domain-mean rain rate during the decay phase of convection through the slowdown in the decrease of perturbation kinetic energy as a result of the exclusion of barotropic conversion from mean kinetic energy to perturbation kinetic energy.

Both liquid and ice clouds are important parts of precipitation systems. Ice clouds are semitransparent to the solar radiation but opaque to the infrared radiation and thus have a strong greenhouse effect. Due to their large optical thickness, liquid clouds reflect most solar radiation back to space and thus have a dominant cooling effect. Xin and Li [8] studied radiative effects of liquid and ice clouds through the analysis of equilibrium cloud-resolving model simulations imposed with zero large-scale vertical velocity. They showed that the exclusion of radiative effects of liquid clouds increases the mean rain rate through the increase in net

**Received** 2017-09-14; **Revised** 2018-06-15; **Accepted** 2018-08-15

**Foundation item:** National Natural Science Foundation of China (41475039, 41775040); National Key Basic Research and Development Project of China (2015CB953601)

**Biography:** LI Xiao-fan, Ph. D., Professor, primarily undertaking research on mesoscale meteorology, cloud microphysics.

**Corresponding author:** LI Xiao-fan, e-mail: xiaofanli@zju.edu.cn

condensation and hydrometeor change from a gain to a loss in the presence of radiative effects of ice clouds and hydrometeor change from a gain to a loss in the absence of radiative effects of ice clouds. The removal of radiative effects of ice clouds increases the mean rain rate via the increase in net condensation regardless of radiative effects of liquid clouds. During the development of pre-summer precipitation systems, strong upward motions and associated heat divergence occur, which may lead to the change in radiative effects on rainfall. Liu et al.[9] revealed that the exclusion of radiative effects of liquid clouds reduces the pre-summer rain rate through the hydrometeor change from a loss to a gain in the presence of radiative effects of ice clouds and the exclusion of radiative effects of liquid clouds increases the pre-summer rain rate through the increase in net condensation and hydrometeor loss in the absence of radiative effects of ice clouds. The increases in net condensation and associated latent heat may correspond to the strengthened infrared radiative cooling in the lower troposphere. The enhanced hydrometeor loss due to the slowdown in the melting of graupel is caused by the strengthened local atmospheric cooling. Shen et al.[10] found that the exclusion of ice clouds weakens the pre-summer rain rate through the substantial reduction in hydrometeor loss in the presence of radiative effects of liquid clouds, but it enhances the pre-summer rain rate through hydrometeor change from a gain to a loss in the absence of radiative effects of ice clouds. The weakened hydrometeor loss corresponds to the enhanced infrared radiative cooling through the increases in condensation, evaporation of rain, depositional growth of snow from cloud ice, collection of cloud ice by snow and accretion of cloud liquid by graupel, and the decreases in collection of cloud liquid by rain and melting of cloud ice to cloud liquid. The hydrometeor change from the gain to the loss is associated with the strengthened infrared radiative cooling in the upper troposphere through the increases in vapor deposition, accretion of cloud liquid by graupel and melting of graupel.

The impacts of ice clouds on the development of convective systems have been intensively studied using cloud-resolving model simulations (e.g., Yoshizaki[11]; Nicholls [12]; Fovell and Ogura [13]; Tao and Simpson[14]; McCumber et al.[15]; Tao et al.[16]; Liu et al.[17]; Grabowski et al. [18]; Wu et al. [19]; Li et al. [20]; Grabowski and Moncrieff [21]; Wu [22]; Grabowski [23]). In additional to radiative effects of ice clouds on rainfall, microphysical processes also have important impacts on rainfall. Ping et al.[24] showed that the elimination of microphysical effects of ice clouds reduces rain rate through the decrease in net condensation and the increase in hydrometeor gain in the absence of radiative effects of ice clouds analyzing the equilibrium sensitivity cloud-resolving model simulations imposed with zero large-scale vertical velocity. Wang et al.[25] conducted sensitivity experiments of pre-summer rainfall and found that the removal of microphysical effects of ice clouds decreases pre-summer rain rate mainly through the hydrometeor change from a loss to a gain.

Domain mean rain rate is a product of rain intensity and fractional rainfall coverage. Li et al.[26] analyzed diurnal cycle of tropical rainfall and revealed that the diurnal cycle of the mean rain rate is associated with diurnal cycle of fractional rainfall coverage because the diurnal variation of rain intensity is significantly weakened through the decrease in rainfall in early morning hours, indicating different radiative effects of rain intensity and fractional rainfall coverage.

The objective of this study is to examine radiative and microphysical effects on the relation between spatial mean rain rate, rain intensity and fractional rainfall coverage using time mean and hourly simulation data of pre-summer torrential rainfall event over the south of China in June 2008. The sensitivity simulation data are briefly described in section 2. The results are presented and discussed in section 3. The summary is given in section 4.

## 2 MODEL, EXPERIMENTS AND ANALYSIS METHODOLOGIES

The data analyzed in this study come from sensitivity simulations conducted by Shen et al.[7, 27] and Wang et al.[25]. The model is integrated from 02:00 LST 3 June to 02:00 LST 8 June 2008 in the control experiment (CTL). The convection with upward motions formed on 4 June 2008, developed on 5 June, and reached its peak with the rainfall amount of 482.2 mm in Yangjiang, Guangdong on 6 June, and then decayed on 7 June (Fig.1a), while westerly winds prevail(Fig 1b). The control experiment has been validated with rain gauge (Wang et al.[25]) and temperature and specific humidity data from National Centers for Environmental Precipitation (NCEP)/Global Data Assimilation System (GDAS) (Shen et al.[7]). Four sensitivity experiments (Table 1a) were carried out. The experiments NWR, NIR and NCR are identical to CTL except that the mixing ratios of liquid hydrometeors (cloud liquid and rain liquid), ice hydrometeors (cloud ice, snow and graupel) and cloud hydrometeors (both liquid and ice hydrometeors) are set to zero when radiation is calculated. The experiment NIM is identical to CTL except for mixing ratios of ice hydrometeors and associated microphysical processes which are set to zero during the model integration. NWR and NCR are respectively compared to CTL and CIR to study radiative effects of liquid clouds on rainfall in the presence (NWR-CTL) and the absence (NCR-NIR) of radiative effects of ice clouds (Table 1b). NIR and NCR are respectively compared to CTL and CWR to study radiative effects of ice clouds on rainfall in the presence (NIR-CTL) and the absence (NCR-NWR) of radiative effects of liquid clouds. NIM is compared to NIR

(NIM-NIR) to study microphysical effects of ice clouds in absence of radiative effects of ice clouds. The control and sensitivity experiment data are used to study radiative and microphysical effects on pre-summer torrential rainfall (Wang et al.[25]; Shen et al.[7, 10, 27-29]; Liu et al.[9]).

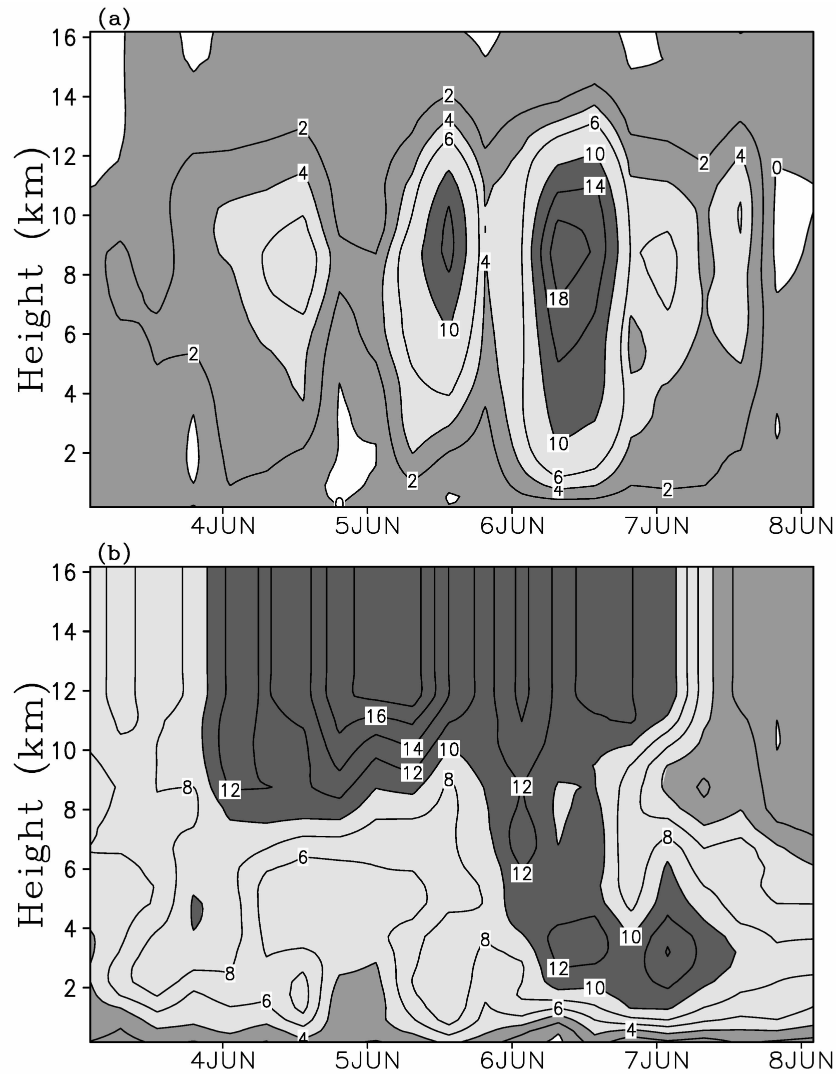


**Figure 1.** Temporal and vertical distribution of (a) vertical velocity (cm $s^{-1}$) and (b) zonal wind (m $s^{-1}$) imposed in the experiments PSR and PSRCO2. Ascending motion in (a) and westerly wind in (b) are shaded.

**Table 1.** Summaries for (a) experiment designs and (b) differences between experiments.

| (a) Exp. | Design |
|---|---|
| CTL | Control experiment in which both liquid and ice hydrometeor mixing ratios are set to non-zero in the calculations of radiation |
| NWR | Liquid hydrometeor mixing ratios are set to zero in the calculations of radiation |
| NIR | Ice hydrometeor mixing ratios are set to zero in the calculations of radiation |
| NCR | Both liquid and ice hydrometeor mixing ratios are set to zero in the calculations of radiation |
| NIM | Ice hydrometeor mixing ratios are set to zero and associated microphysical processes are removed |
| (b) | The effects to be studied |
| NWR-CTL | Radiative effects of liquid clouds on rainfall in the presence of radiative effects of ice clouds |
| NCR-NIR | Radiative effects of liquid clouds on rainfall in the absence of radiative effects of ice clouds |
| NIR-CTL | Radiative effects of ice clouds on rainfall in the presence of radiative effects of liquid clouds |
| NCR-NWR | Radiative effects of ice clouds on rainfall in the absence of radiative effects of liquid clouds |
| NIM-NIR | Microphysical effects of ice clouds on rainfall in the absence of radiative effects of liquid clouds |

Shen et al. [7, 27] and Wang et al. [25] used the two-dimensional cloud-resolving model (Soong and Ogura[30]; Soong and Tao[31]; Tao and Simpson[32]; Sui et al.[33, 34]; Li et al.[20, 35]). The model (Li and Gao[36, 37]) with periodic boundary conditions containing prognostic equations for perturbation momentum, potential temperature, specific humidity, cloud liquid, raindrops, cloud ice, snow and graupel. The source/sink terms in specific humidity and cloud equations are calculated from cloud microphysical parameterization schemes (Lin et al. [38]; Rutledge and Hobbs [39, 40]; Tao et al. [41]; Krueger et al. [42]). The source/sink terms in thermodynamic equation are computed from solar and infrared radiative parameterization schemes (Chou and Suarez [43]; Chou et al.[44, 45]). The basic model parameters include grid mesh of 1.5 km with 512 grid point long zonal direction, a time step of 12 s, and 33 vertical levels with the grid mesh of 200 m near the surface and 1 km in the upper troposphere. The two-dimensional framework is used in this study due to similarities in two- and three-dimensional model simulations in terms of thermodynamics, surface heat fluxes, rainfall, precipitation efficiency, and vertical transports of mass, sensible heat, and moisture (e.g., Tao and Soong [46]; Tao et al. [47]; Grabowski et al. [48]; Tompkins [49]; Khairoutdinov and Randall [50]; Sui et al. [51]). The main difference in 2D and 3D model simulations is the difference in dynamics. Gao et al.[52] and Gao[53] revealed that the horizontal and vertical components of the dynamic vorticity vector are highly correlated with cloud hydrometeors, respectively, in 3D and 2D frameworks since dominant items in horizontal components of the 3D dynamic vorticity vector are excluded from the 2D framework.

Following Li et al. [26], model domain mean rain rate is a product of rain intensity (RI; rain rate average over rainfall area) and fractional rainfall coverage (FRC; the ratio of rain grids to total model domain grids), i.e.,

$$P_S = \mathrm{RI} \times \mathrm{FRC}. \quad (1)$$

Based on (1), the difference in $P_S(y)$ and $P_S(x)$ caused by the exclusion of radiative effects of liquid or ice clouds can be written as

$$P_S(y) - P_S(x) = \mathrm{RI}(y)\mathrm{FRC}(y) - \mathrm{RI}(x)\mathrm{FRC}(x) = [\mathrm{RI}(y) - \mathrm{RI}(x)][\mathrm{FRC}(y) - \mathrm{FRC}(x)] + \mathrm{RI}(x)[\mathrm{FRC}(y) - \mathrm{FRC}(x)] + \mathrm{FRC}(x)[\mathrm{RI}(y) - \mathrm{RI}(x)]. \quad (2)$$

Here $(y, x)$=(NWR, CTL), (NCR, NIR), (NIR, CTL), (NCR, NWR).

The convective-stratiform rainfall is separated using the scheme developed by Tao et al. [54] and modified by Sui et al. [33]. Model grid points in the two-dimensional surface rain field that have a rain rate twice as large as the average taken over the surrounding four grid points are identified as the cores of convective cells. For each core grid point, the grid point on either side along the zonal direction is also considered convective. In addition, any grid point with a rain rate of 20 mm h$^{-1}$ or more is designated as convective regardless of the above criteria. All non-convective rainfall points are regarded as stratiform. Other criteria such as a maximum updraft above 600 hPa and cloud liquid are also used to detect convective rainfall.

## 3 RESULTS

In this section, cloud radiative effects on the relation between domain mean rain rate, RI and FRC are first analyzed using time mean simulation data. The exclusion of radiative effects of liquid and ice clouds reduces domain mean rain rate, respectively, from CTL to NWR and from CTL to NIR through the decrease in RI (Table 2a). The removal of radiative effects of liquid and ice clouds increases domain mean rain rate, respectively, from NIR to NCR and from NWR to NCR through the increase in RI. The elimination of microphysical effects of ice clouds decreases domain mean rain rate from NIR to NIM via the shrink in FRC as a result of severely damaged stratiform clouds.

Like radiative effects on domain mean rain rate, the removal of radiative effects of liquid and ice clouds increases convective rain rate, respectively, from NIR to NCR and from NWR to NCR through the increase in RI. Unlike radiative effects on domain mean rain rate, the exclusion of radiative effects of liquid clouds reduces convective rain rate from CTL to NWR mainly through the shrink in FRC (Table 3a), whereas the removal of radiative effects of ice clouds barely changes convective rain rate in CTL and NIR (absolute difference in rain rate is less than 0.01 mm h-1) due to the offset between the shrink in FRC and the increase in RI from CTL to NIR. The elimination of microphysical effects of ice clouds increases convective rain rate from NIR to NIM due to the fact that the expansion in fractional rainfall convergence overcomes the reduction in RI.

The exclusion of radiative effects of liquid clouds barely changes stratiform rain rate regardless of radiative effects of ice clouds due to the cancellation between the expansion in FRC and the reduction in RI from CTL to NWR and similar RI and FRC in NIR and NCR (Table 4a). The removal of radiative effects of ice clouds decreases stratiform rain rate regardless of radiative effects of liquid clouds due to the reduction in RI from CTL to NIR and the shrink in FRC and the weakening in RI from NWR to NCR. The elimination of microphysical effects of ice clouds decreases stratiform rain rate from NIR to NIM due to the shrink in FRC.

Although the evolution of domain mean rain rate is generally controlled by imposed large-scale vertical velocity, cloud radiative and microphysical processes show impacts on domain mean rain rate, RI and FRC (Fig.2). The standard deviations of difference in domain mean rain rate, rain intensity and fractional rainfall coverage are generally one order of magnitude larger than the differences in their time means of NWR-CTL, NCR-NIR, NIR-CTL and NCR-NWR whereas they have similar magnitudes to their time means for NIM-NIR (Table 5). This indicates a large cancellation between cloud radiative and microphysical effects at hourly time scale on the change in domain mean rain rate, rain intensity and fractional rainfall coverage.

**Table 2.** Differences in domain mean rain rate ($P_S$) for NWR-CTL, NCR-NIR, NIR-CTL, NCR-NWR and NIM-NIR and their decompositions ($P_{S1}$, $P_{S2}$, $P_{S3}$) calculated using (a) time-mean rain-rate difference data, and (b) negative and (c) positive rain-rate difference data. Unit is mm $h^{-1}$.

| (a) | NWR-CTL | NCR-NIR | NIR-CTL | NCR-NWR | NIM-NIR |
|---|---|---|---|---|---|
| $P_S$ | −0.043 | 0.061 | −0.043 | 0.061 | −0.166 |
| $P_{S1}$ | −0.006 | 0.000 | −0.001 | −0.005 | −0.297 |
| $P_{S2}$ | 0.083 | 0.006 | 0.015 | −0.057 | −0.606 |
| $P_{S3}$ | −0.120 | 0.055 | −0.057 | 0.123 | 0.737 |
| (b) | NWR-CTL | NCR-NIR | NIR-CTL | NCR-NWR | NIM-NIR |
| $P_S$ | −0.261 | −0.214 | −0.241 | −0.174 | −0.360 |
| $P_{S1}$ | 0.013 | 0.014 | 0.015 | 0.010 | −0.058 |
| $P_{S2}$ | −0.047 | −0.094 | −0.064 | −0.063 | −0.434 |
| $P_{S3}$ | −0.227 | −0.135 | −0.192 | −0.120 | 0.132 |
| (c) | NWR-CTL | NCR-NIR | NIR-CTL | NCR-NWR | NIM-NIR |
| $P_S$ | 0.218 | 0.275 | 0.198 | 0.234 | 0.194 |
| $P_{S1}$ | 0.014 | 0.021 | 0.011 | −0.001 | −0.194 |
| $P_{S2}$ | 0.117 | 0.077 | 0.062 | −0.004 | −0.178 |
| $P_{S3}$ | 0.086 | 0.176 | 0.126 | 0.239 | 0.565 |

**Table 3.** As in Table 2 except for convective rain rate.

| (a) | NWR-CTL | NCR-NIR | NIR-CTL | NCR-NWR | NIM-NIR |
|---|---|---|---|---|---|
| $P_S$ | −0.048 | 0.052 | −0.004 | 0.096 | 0.036 |
| $P_{S1}$ | 0.000 | 0.000 | −0.006 | −0.005 | −0.037 |
| $P_{S2}$ | −0.035 | 0.010 | −0.079 | 0.034 | 0.238 |
| $P_{S3}$ | −0.014 | 0.041 | 0.081 | 0.135 | −0.165 |
| (b) | NWR-CTL | NCR-NIR | NIR-CTL | NCR-NWR | NIM-NIR |
| $P_S$ | −0.249 | −0.203 | −0.212 | −0.154 | −0.245 |
| $P_{S1}$ | 0.028 | 0.018 | 0.021 | 0.011 | −0.013 |
| $P_{S2}$ | −0.084 | −0.100 | −0.112 | −0.101 | 0.030 |
| $P_{S3}$ | −0.193 | −0.120 | −0.122 | −0.065 | −0.261 |
| (c) | NWR-CTL | NCR-NIR | NIR-CTL | NCR-NWR | NIM-NIR |
| $P_S$ | 0.201 | 0.254 | 0.209 | 0.250 | 0.281 |
| $P_{S1}$ | 0.011 | 0.028 | 0.005 | 0.015 | 0.026 |
| $P_{S2}$ | 0.037 | 0.068 | 0.011 | 0.033 | 0.190 |
| $P_{S3}$ | 0.152 | 0.158 | 0.193 | 0.202 | 0.065 |

**Table 4.** As in Table 2 except for stratiform rain rate.

| (a) | NWR-CTL | NCR-NIR | NIR-CTL | NCR-NWR | NIM-NIR |
|---|---|---|---|---|---|
| $P_S$ | 0.005 | 0.009 | −0.039 | −0.035 | −0.202 |
| $P_{S1}$ | −0.002 | 0.000 | −0.001 | 0.001 | −0.042 |
| $P_{S2}$ | 0.036 | 0.001 | 0.014 | −0.020 | −0.238 |
| $P_{S3}$ | −0.028 | 0.008 | −0.051 | −0.016 | 0.077 |
| (b) | NWR-CTL | NCR-NIR | NIR-CTL | NCR-NWR | NIM-NIR |
| $P_S$ | −0.087 | −0.094 | −0.118 | −0.103 | −0.218 |
| $P_{S1}$ | 0.005 | 0.005 | 0.007 | 0.011 | −0.019 |
| $P_{S2}$ | −0.023 | −0.015 | −0.023 | −0.046 | −0.233 |
| $P_{S3}$ | −0.069 | −0.083 | −0.102 | −0.067 | 0.035 |
| (c) | NWR-CTL | NCR-NIR | NIR-CTL | NCR-NWR | NIM-NIR |
| $P_S$ | 0.092 | 0.103 | 0.079 | 0.068 | 0.016 |
| $P_{S1}$ | 0.009 | 0.006 | 0.008 | 0.005 | −0.011 |
| $P_{S2}$ | 0.048 | 0.012 | 0.025 | 0.020 | −0.007 |
| $P_{S3}$ | 0.035 | 0.085 | 0.046 | 0.044 | 0.035 |

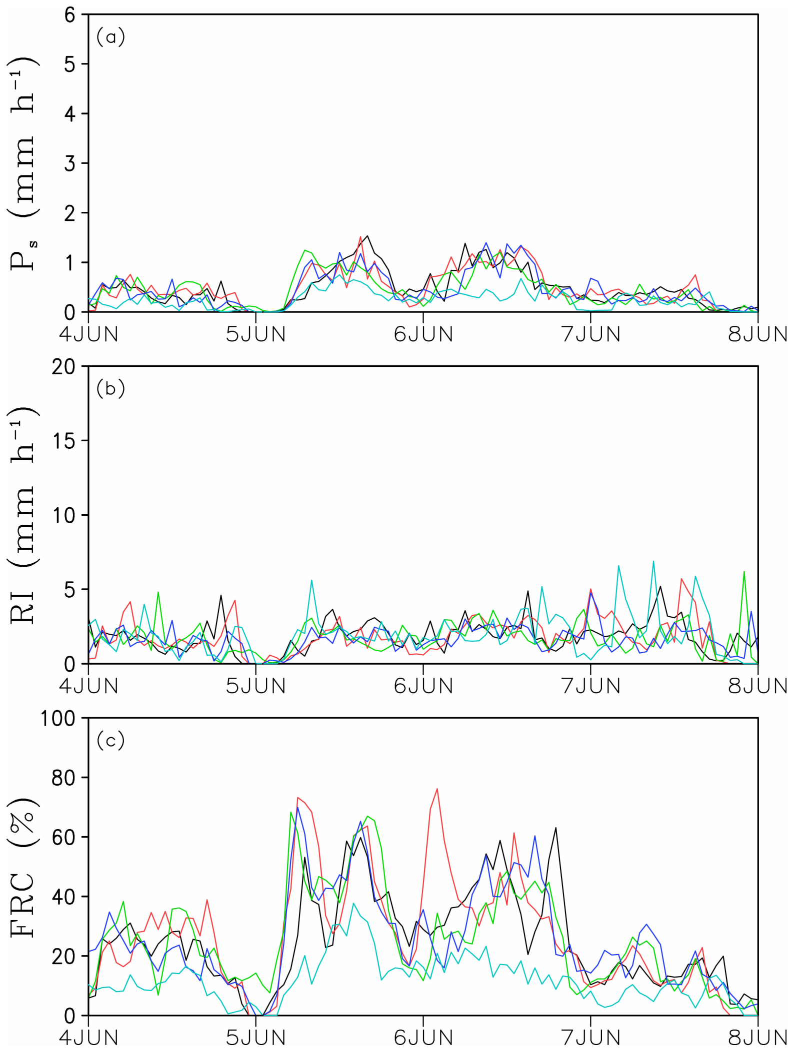


**Figure 2.** (a) Domain mean surface rain rate (PS; mm h$^{-1}$), (b) rain intensity (RI; mm h$^{-1}$) and (c) fractional rainfall coverage (FRC; %) in CTL (black), NWR (red), NIR (green), NCR (blue) and NIM (cyan).

**Table 5.** (a) Time means and (b) standard deviations of model domain mean rain rate (PS; mm h$^{-1}$), rain intensity (RI; mm h$^{-1}$) and fractional rainfall coverage (FRC; %) for NWR-CTL, NCR-NIR, NIR-CTL, NCR-NWR and NIM-NIR.

| (a) | NWR-CTL | NCR-NIR | NIR-CTL | NCR-NWR | NIM-NIR |
|---|---|---|---|---|---|
| $P_S$ | −0.043 | 0.061 | −0.043 | 0.061 | −0.166 |
| $RI$ | −0.026 | −0.071 | −0.109 | −0.154 | 0.213 |
| $FRC$ | 1.9 | 0.1 | 0.7 | −1.1 | −14.0 |
| (b) | NWR-CTL | NCR-NIR | NIR-CTL | NCR-NWR | NIM-NIR |
| $P_S$ | 0.627 | 0.638 | 0.621 | 0.555 | 0.698 |
| $RI$ | 1.228 | 1.201 | 1.338 | 1.062 | 1.681 |
| $FRC$ | 13.6 | 9.0 | 12.3 | 12.7 | 12.5 |

Thus, we take the summation for positive and negative difference separately and found that the magnitudes of positive and negative differences are significantly larger than the difference in time mean and they largely cancel out each other (Tables 2-4). The comparison between CTL and NWR shows that while the rainfall areal expansion is larger than the shrink, the reduced RI is about three times larger than the enhanced RI, which leads to the decrease in time mean rain rate (Table 2). While the rainfall areal expansion is smaller than the shrink, the reduced RI is stronger than the enhanced RI, slowing down convective rainfall (Table 3). Over stratiform regions, the rainfall areal shrink is smaller than the rainfall areal expansion, while the reduced RI is stronger than the enhanced RI (Table 4); their cancellation leads to the insensitivity of stratiform rain rate to radiative processes of liquid clouds in the presence of radiative effects of ice clouds.

The comparison between NIR and NCR reveals that while the rainfall areal expansion is slightly smaller than the shrink, the enhanced RI is larger than the reduced RI, which leads to the increase in domain mean rain rate and convective rain rate (Tables 2 and 3). Over stratiform regions, the rainfall areal shrink and the reduced RI are respectively cancelled out by the rainfall areal expansion and the enhanced RI (Table 4), which causes stratiform rainfall insensitive to radiative processes of liquid clouds in the absence of radiative effects of ice clouds.

While the rainfall area is not sensitive to radiative processes of ice clouds in the presence of radiative effects of liquid clouds, the reduced RI from CTL to NIR is stronger than the enhanced RI, which decreases domain mean rain rate and stratiform rain rate (Tables 2 and 4) . Over convective regions, the rainfall areal shrink is larger than the expansion, but the reduced RI is weaker than the enhanced RI (Table 3); both effects are cancelled out each other, which maintains convective rain rate.

When radiative effects of ice clouds are excluded, the enhanced RI from NWR to NCR is twice stronger than the reduced RI in the absence of radiative effects of liquid clouds (Table 2), increasing domain mean rain rate. Over convective regions, although the rainfall areal shrink is larger than the expansion, the enhanced RI is three times stronger than the reduced RI (Table 3), strengthening convective rain rate. Over stratiform regions, the rainfall areal shrink is larger than the expansion, and the reduced RI is stronger than the enhanced RI (Table 4), which reduces stratiform rain rate.

When microphysical effects of ice clouds are removed, domain mean rain rate and stratiform rain rate are reduced from NIR to NIM due to both the reduced RI and the rainfall areal shrink (Tables 2 and 4). Over convective regions, the rainfall areal expansion causes the slight increase in convective rain rate (Table 3).

The difference in rainfall caused by cloud radiative processes can be further analyzed with mass-weighted vertically integrated surface rainfall budget, which is expressed by

$$P_S=Q_{NC}+Q_{CM}, \quad (3)$$

where $P_S$ is rain rate, $Q_{NC}$ is net condensation, and $Q_{CM}$ is hydrometeor change/convergence. Domain mean of $Q_{CM}$ is hydrometeor change since hydrometeor convergence vanishes as a result of lateral boundaries of cloud resolving model. Positive $Q_{NC}$ denotes net condensation, whereas negative $Q_{NC}$ is net evaporation. Positive $Q_{CM}$ denotes hydrometeor loss/convergence, whereas negative $Q_{CM}$ is hydrometeor gain/divergence.

The reductions in domain mean rain rate are associated with the hydrometeor change from a loss in CTL to a gain in NWR, the decrease in hydrometeor loss from CTL and NIR, and the hydrometeor change from a weak loss in NIR to a strong gain in NIM, respectively (Tables 6a and 6b). The increases in domain mean rain rate correspond to the enhancement in net condensation from NIR to NCR and the hydrometeor change from a gain in NWR to a loss in NCR. The increase in net condensation from NIR to NCR is associated with enhanced release of latent heat in the lower troposphere in response to the strengthened infrared cooling as a result of the exclusion of radiative effects of water clouds in the absence of radiative effects of ice clouds (Liu et al.[9]).

The reduction in convective rain rate from CTL to NWR is related to the intensification in hydrometeor gain over convective regions (Tables 6c and 6d). The increases in convective rain rate are associated with the enhancement in net condensation from NIR to NCR and from NWR to NCR, and the suppression in hydrometeor gain from NIR to NIM. The similar convective rain rates in CTL and NIR are related to the cancellation between the enhancement in net condensation and the enhancement in hydrometeor gain.

**Table 6.** Surface rainfall budget [rain rate ($P_S$), net condensation ($Q_{NC}$) and hydrometeor change ($Q_{CM}$)] for (a) (c) (e) CTL, NWR, NIR, NCR and NIM and (b) (d) (f) their differences for NWR-CTL, NCR-NIR, NIR-CTL, NCR-NWR and NIM-NIR averaged over (a) (b) model domain, and (c) (d) convective and (e) (f) stratiform regions using time-mean simulation data. Unit is mm h$^{-1}$.

| (a) | CTL | NWR | NIR | NCR | NIM |
|---|---|---|---|---|---|
| $P_S$ | 1.546 | 1.503 | 1.503 | 1.563 | 1.337 |
| $Q_{NC}$ | 1.508 | 1.534 | 1.500 | 1.548 | 1.473 |
| $Q_{CM}$ | 0.038 | −0.031 | 0.002 | 0.016 | −0.136 |
| (b) | NWR-CTL | NCR-NIR | NIR-CTL | NCR-NWR | NIM-NIR |
| $P_S$ | −0.043 | 0.061 | −0.043 | 0.061 | −0.166 |
| $Q_{NC}$ | 0.026 | 0.047 | −0.007 | 0.014 | −0.028 |
| $Q_{CM}$ | −0.069 | 0.013 | −0.036 | 0.047 | −0.138 |
| (c) | CTL | NWR | NIR | NCR | NIM |
| $P_S$ | 1.068 | 1.019 | 1.064 | 1.115 | 1.100 |
| $Q_{NC}$ | 1.308 | 1.342 | 1.374 | 1.440 | 1.285 |
| $Q_{CM}$ | −0.240 | −0.323 | −0.311 | −0.324 | −0.185 |
| (d) | NWR-CTL | NCR-NIR | NIR-CTL | NCR-NWR | NIM-NIR |
| $P_S$ | −0.048 | 0.052 | −0.004 | 0.096 | 0.036 |
| $Q_{NC}$ | 0.034 | 0.065 | 0.066 | 0.098 | −0.090 |
| $Q_{CM}$ | −0.082 | −0.014 | −0.070 | −0.002 | 0.126 |
| (e) | CTL | NWR | NIR | NCR | NIM |
| $P_S$ | 0.478 | 0.483 | 0.439 | 0.448 | 0.237 |
| $Q_{NC}$ | 0.200 | 0.192 | 0.127 | 0.108 | 0.189 |
| $Q_{CM}$ | 0.278 | 0.291 | 0.312 | 0.340 | 0.048 |
| (f) | NWR-CTL | NCR-NIR | NIR-CTL | NCR-NWR | NIM-NIR |
| $P_S$ | 0.005 | 0.009 | −0.039 | −0.035 | −0.202 |
| $Q_{NC}$ | −0.008 | −0.019 | −0.074 | −0.084 | 0.062 |
| $Q_{CM}$ | 0.013 | 0.028 | 0.035 | 0.049 | −0.264 |

The similar stratiform rainfall budgets lead to the similar stratiform rain rates in CTL and NWR and in NIR and NCR (Tables 6e and 6f). The reductions in stratiform rain rate correspond to the decreases in net condensation from CTL to NIR and from NWR to NCR over stratiform regions and the large suppression in hydrometeor loss from NIR to NIM.

## 4 SUMMARY

Spatial mean rain rate is a product of rain intensity and fractional rainfall coverage. Cloud radiative effects on the relation between spatial mean rain rate, rain intensity and fractional rainfall coverage are investigated using time-mean and hourly sensitivity experiment data of pre-summer heavy rainfall over the south of China during June 2008. The main results from the analysis of time-mean data include:

(1) The exclusion of radiative effects of liquid clouds reduces domain mean rain rate by decreasing convective rain rate mainly through the shrink in fractional rainfall coverage as a result of the increase in hydrometeor gain over convective regions in the presence of radiative effects of ice clouds. The exclusion of radiative effects of liquid clouds increases

domain mean rain rate by increasing convective rain rate mainly via the strengthening in rain intensity associated with the increase in net condensation over convective regions in the absence of radiative effects of ice clouds.

(2) The removal of radiative effects of ice clouds decreases domain mean rain rate by reducing stratiform rain rate through the suppression in rain intensity related to the reduction in net condensation over stratiform regions in the presence of radiative effects of liquid clouds. The removal of radiative effects of ice clouds increases domain mean rain rate by strengthening convective rain rate mainly via the enhancement in rain intensity in response to the increase in net condensation over convective regions in the absence of radiative effects of liquid clouds.

(3) The elimination of microphysical effects of ice clouds suppresses domain mean rain rate by reducing stratiform rain rate through the shrink in fractional rainfall coverage over stratiform rainfall regions as a result of severely damaged stratiform clouds.

***Acknowledgement:*** The authors thank TAO W K at NASA/GSFC for his cloud-resolving model and the support from the training center of atmospheric sciences of Zhejiang University.

**REFERENCES:**

[1] KRISHNAMURTI T N, MOLINARI J, PAN H L. Numerical simulation of the Somali Jet [J]. J Atmos Sci, 1976, 33(12): 2350-2362.

[2] TAO S, DING Y. Observational evidence of the influence of the Qinghai-Xizang (Tibet) plateau on the occurrence of heavy rain and severe convective storms in China [J]. Bull Amer Meteor Soc, 1981, 62(1): 23-30.

[3] WANG J, LI M. Cross equator flow from Australia and summer monsoon circulations and precipitation over China [J]. Sci Atmos Sinica, 1982, 6(1): 1-10.

[4] DING Yi-hui. East Asia Monsoon [M]. Beijing: China Meteorological Press, 1994: 1-263.

[5] SIMMONDS I, BI I D, HOPE P. Atmospheric liquid vapor flux and its association with rainfall over China in summer [J]. J Climate, 1999, 12(5): 1353-1367.

[6] LOU Xiao-feng, HU Zhi-jin, SHI Yue-qin, et al. Numerical simulations of a heavy rainfall case in south China [J]. Adv Atmos Sci, 2003, 20(1): 128-138.

[7] SHEN X, WANG Y, LI X. Radiative effects of liquid clouds on precipitation rate responses to the large-scale forcing during pre-summer heavy precipitation rate over southern China [J]. Atmos Res, 2011, 99(1): 120-128.

[8] XIN J, LI X. Precipitation responses to radiative processes of liquid and ice clouds: An equilibrium cloud-resolving modeling study [J]. Atmos Oceanic Sci Lett, 2016, 9(4): 306-314.

[9] LIU J, SHEN X, LI X. 2014: Radiative effects of liquid clouds on heat, cloud microphysical and surface precipitation rate budgets associated with pre-summer torrential precipitation rate [J]. Terres Atmos Oceanic Sci, 2014, 25(1): 41-50.

[10] SHEN Xin-yong, HUANG Wen-yan, GUO Chun-yan, et al. Precipitation responses to radiative effects of ice clouds: A cloud-resolving modeling study of a pre-summer torrential precipitation event [J]. Adv Atmos Sci, 2016, 33(5): 1137-1142.

[11] YOSHIZAKI M. Numerical simulations of tropical squall-line clusters: Two-dimensional model [J]. J Meteor Soc Japan, 1986, 64(4): 469-491.

[12] NICHOLLS M E. A comparison of the results of a two-dimensional numerical simulation of a tropical squall line with observations [J]. Mon Wea Rev, 1987, 115(12): 3055-3077.

[13] FOVELL R G, OGURA Y. Numerical simulation of a midlatitude squall line in two dimensions [J]. J Atmos Sci, 1988, 45(24): 3846-3879.

[14] TAO W K, SIMPSON J. Modeling study of a tropical squall-type convective line [J]. J Atmos Sci, 1989, 46(2): 177-202.

[15] McCUMBER M, TAO W K, SIMPSON J, et al. Comparison of ice-phase microphysical parameterization schemes using numerical simulations of tropical convection [J]. J Appl Meteor, 1991, 30(7): 985-1004.

[16] TAO W K, SIMPSON J, SOONG S T. Numerical simulation of a subtropical squall line over the Taiwan Strait [J]. Mon Wea Rev, 1991, 119(11): 2699-2723.

[17] LIU C, MONCRIEFF M W, ZIPSER E J. Dynamic influence of microphysics in tropical squall lines: A numerical study [J]. Mon Wea Rev, 1997, 125 (9): 2193-2210.

[18] GRABOWSKI W W, WU X, MONCRIEFF M W. Cloud-resolving model of tropical cloud systems during Phase III of GATE. Part III: Effects of cloud microphysics [J]. J Atmos Sci, 1999, 56(14): 2384-2402.

[19] WU X, HALL W D, GRABOWSKI W W, et al. Long-term behavior of cloud systems in TOGA COARE and their interactions with radiative and surface processes. Part II: Effects of ice microphysics on cloud-radiation interaction [J]. J Atmos Sci, 1999, 56(18): 3177-3195.

[20] LI X, SUI C H, LAU K M, et al. Large-scale forcing and cloud-radiation interaction in the tropical deep convective regime [J]. J Atmos Sci, 1999, 56(17): 3028-3042.

[21] GRABOWSKI, W W, MONCRIEFF M W. Large-scale organization of tropical convection in two-dimensional explicit numerical simulations [J]. Quart J Roy Meteor Soc, 2001, 127(2): 445-468.

[22] WU X. Effects of ice microphysics on tropical radiative-convective-oceanic quasi-equilibrium states [J]. J Atmos Sci, 2002, 59(11): 1885-1897.

[23] GRABOWSKI W W. Impact of ice microphysics on multiscale organization of tropical convection in two-dimensional cloud-resolving simulations [J]. Quart J Roy Meteor Soc, 2003, 129(1): 67-81.

[24] PING F, LUO Z, LI X. Microphysical and radiative effects of ice microphysics on tropical equilibrium states: A two-dimensional cloud-resolving modeling study [J]. Mon Wea Rev, 2007, 135(7): 2794-2802.

[25] WANG Y, SHEN X, LI X. Microphysical and radiative effects of ice clouds on responses of rainfall to the large-scale forcing during pre-summer heavy rainfall over southern China [J]. Atmos Res, 2010, 97(1): 35-46.

[26] LI X, ZHAI G, ZHU, LIU R. An equilibrium cloud-resolving modeling study of diurnal variation of

tropical rainfall [J]. Dyn Atmos Ocean, 2015, 71 (1): 108-117.
[27] SHEN X, WANG Y, LI X. Effects of vertical wind shear and cloud radiative processes on responses of precipitation rate to the large-scale forcing during pre-summer heavy precipitation rate over southern China [J]. Quart J Roy Meteor Soc, 2011, 137(1): 236-249.
[28] SHEN, X, ZHANG N, LI X. Effects of large-scale forcing and ice clouds on pre-summer heavy precipitation rate over southern China in June 2008: A partitioning analysis based on surface precipitation rate budget [J]. Atmos Res, 2011, 101(1): 155-163.
[29] SHEN Xin-yong, LIU Jia, LI Xiao-fan. Torrential precipitation rate responses to ice microphysical processes during pre-summer heavy precipitation rate over southern China [J]. Adv Atmos Sci, 2012, 29 (3): 493-500.
[30] SOONG S T, OGURA Y. Response of tradewind cumuli to large-scale processes [J]. J Atmos Sci, 1980, 37 (9): 2035-2050.
[31] SOONG S T, TAO W K. Response of deep tropical cumulus clouds to Mesoscale processes [J]. J Atmos Sci, 1980, 37(9): 2016-2034.
[32] TAO W K, SIMPSON J. The Goddard Cumulus Ensemble model. Part I: Model description [J]. Terr Atmos Oceanic Sci, 1993, 4(1): 35-72.
[33] SUI C H, LAU K M, TAO W K, et al. The tropical liquid and energy cycles in a cumulus ensemble model. Part I: Equilibrium climate [J]. J Atmos Sci, 1994, 51 (5): 711-728.
[34] SUI C H, LI X, LAU K M. Radiative-convective processes in simulated diurnal variations of tropical oceanic convection [J]. J Atmos Sci, 1998, 55 (14): 2345-2359.
[35] LIX, SUI C H, LAU K M. Dominant cloud microphysical processes in a tropical oceanic convective system: A 2-D cloud resolving modeling study [J]. Mon Wea Rev, 2002, 130(10): 2481-2491.
[36] LI X, GAO S. Precipitation Modeling and Quantitative Analysis [M]. Dordrecht: Springer. 2011: 1-240.
[37] LI X, GAO S. Cloud-resolving Modeling of Convective Processes [M]. 2nd edition, Switzerland: Springer, 2016: 1-355.
[38] LIN Y L, FARLEY R D, ORVILLE, H D. Bulk parameterization of the snow field in a cloud model [J]. J Climate Appl Meteor, 1983, 22(6): 1065-1092.
[39] RUTLEDGE S A, HOBBS P V. The mesoscale and microscale structure and organization of clouds and precipitation in midlatitude cyclones. Part VIII: A model for the "seeder-feeder" process in warm-frontal rainbands [J]. J Atmos Sci, 1983, 40(5): 1185-1206.
[40] RUTLEDGE S A, HOBBS P V. The mesoscale and microscale structure and organization of clouds and precipitation in midlatitude cyclones. Part XII: A diagnostic modeling study of precipitation development in narrow cold-frontal rainbands [J]. J Atmos Sci, 1984, 41(20): 2949-2972.
[41] TAO W K, SIMPSON J, McCUMBER M. An ice-liquid saturation adjustment [J]. Mon Wea Rev, 1989, 117(1): 231-235.
[42] KRUEGER S K, FU Q, LIOU K N, et al. Improvement of an ice-phase microphysics parameterization for use in numerical simulations of tropical convection [J]. J Appl Meteor, 1995, 34(1): 281-287.
[43] CHOU M D, SUAREZ M J. An efficient thermal infrared radiation parameterization for use in general circulation model [R]. NASA Tech Memo 104606 (3), 1994: 1-85. [Available from NASA/Goddard Space Flight Center, Code 913, Greenbelt, MD 20771.]
[44] CHOU M D, KRATZ D P, RIDGWAY W. Infrared radiation parameterization in numerical climate models [J]. J Climate, 1991, 4(4): 424-437.
[45] CHOU M D, SUAREZ M J, HO C H, et al. Parameterizations for cloud overlapping and shortwave single scattering properties for use in general circulation and cloud ensemble models [J]. J Atmos Sci, 1998, 55 (2): 201-214.
[46] TAO W K, SOONG S T. The study of the response of deep tropical clouds to mesoscale processes: Three-dimensional numerical experiments [J]. J Atmos Sci, 1986, 43(22): 2653-2676.
[47] TAO W K, SIMPSON J, SOONG S T. Statistical properties of a cloud ensemble: A numerical study [J]. J Atmos Sci, 1987, 44(21): 3175-3187.
[48] GRABOWSKI W W, WU X, MONCRIEFF M W, et al. Cloud-resolving model of tropical cloud systems during Phase III of GATE. Part II: Effects of resolution and the third spatial dimension [J]. J Atmos Sci, 1998, 55(22): 3264-3282.
[49] TOMPKINS A M. The impact of dimensionality on long-term cloud-resolving model simulations [J]. Mon Wea Rev, 2000, 128(5): 1521-1535.
[50] KHAIROUTDINOV M F, RANDALL D A. Cloud-resolving modeling of the ARM summer 1997 IOP: Model formulation, results, uncertainties, and sensitivities [J]. J Atmos Sci, 2003, 60(4): 607-625.
[51] SUI C H, LI X, YANG M J, et al. Estimation of oceanic precipitation efficiency in cloud models [J]. J Atmos Sci, 2005, 62(12): 4358-4370.
[52] GAO S, CUI X, ZHOU Y, et al. A modeling study of moist and dynamic vorticity vectors associated with 2D tropical convection [J]. J Geophys Res, 2005, 110(D17), doi:10.1029/2004JD005675.
[53] GAO S, LI X, TAO W K, et al. Convective and moist vorticity vectors associated with three-dimensional tropical oceanic convection during KWAJEX [J] J Geophys Res, 2007, 112(D14), doi:10.1029/2006JD7179.
[54] TAO W K, SIMPSON J, SUI C H, et al. Heating, moisture and liquid budgets of tropical and midlatitude squall lines: Comparisons and sensitivity to longwave radiation [J]. J Atmos Sci, 1993, 50(5): 673-690.

**Citation:** ZHANG Xiao-yi, ZHANG Zi-han and LI Xiao-fan. Cloud radiative and microphysical effects on the relation between spatial mean rain rate, rain intensity and fractional rainfall coverage [J]. J Trop Meteor, 2018, 24(3): 346-355.